Construction and Building Materials 259 (2020) 120393

Contents lists available at ScienceDirect

Construction and Building Materials

journal homepage: www.elsevier.com/locate/conbuildmat

Effect of the particle size of nanosilica on early age compressive strength in oil-well cement paste

Mtaki Thomas Maagi, Gu Jun *

Department of Petroleum Engineering, Faculty of Earth Resources, China University of Geosciences, Wuhan 430074, China

HIGHLIGHTS

- Nanosilica significantly increases oil-well cement's early compressive strength.
- The improvement in strength relied on the particle sizes of nanosilica.
- Medium-sized nanosilica with a particle size of 40 nm was the best result in a pozzolanic activity.
- Microscopic analysis tests are in good agreement with hardened cement paste compressive strength results.

ARTICLE INFO

Article history:
Received 8 January 2020
Received in revised form 26 June 2020
Accepted 29 June 2020

Keywords:
Oil-well cement
Nanosilica
Early compressive strength
Hardened cement

ABSTRACT

This study evaluates the early compressive strength of oil-well cement pastes containing nanosilica (NS) with different particle sizes of 10, 20 and 40 nm. The NS particles were chosen at proportions corresponding to 1, 2, 3 and 4% by weight of cement. Test results indicated that NS significantly enhanced the early compressive strength of the oil-well cement. The results also revealed that the strength enhancement was reliant on the NS particle sizes. The specimens containing NS 40 nm received greater early compressive strength and higher pozzolanic activity due to better dispersion, resulting in improved microstructures compared with specimens containing 10 and 20 nm. By fluctuating the NS dosages, the optimal replacement dosage was 3% for all particle sizes. This implies that the particle size did not affect the optimal dosage of NS, it influenced the compressive strength of cement paste. The microscopic analysis tests confirmed the findings of the compressive strength of the hardened cement paste.

1. Introduction

Formation fluid leakage has been proclaimed as a major challenge problem in oil and gas wells for a long period. The fluid leaking is correlated with the fluid movement through the wellbore's cemented annulus section. Implications of fluid leakages into the wellbore include increased costs of remedy and production, as well as environmental consequences [1,2]. Some experiments have shown that poor interaction between cement and rock leads to the leakage of fluids from the formation. Cement performance and properties therefore need to be improved to obtain a high strength bond between cement and formation. According to Nelson and Guillot [3], a well lacking a good cement job could never accomplish its total production potential. Therefore, to gain maximum turnover from the well, it is necessary to establish high strength and durable cement structures for long-term zonal isolation. In addition, Nelson and Guillot [3] proposed changing oil-well cement to improve its functionalities. In that regard, various researchers in recent years have concentrated on the use of materials that can provide high performance to boost the useful lifespan of the well and to reduce costs interrelated with the renovation or losses due to failures in the cement sheath. One of these materials is nanosilica (NS), currently used extensively throughout the world in cement-related research.

Because of its nano-scale size, NS has exceptional properties that fundamentally vary with its macro-sized counterparts [4]. In addition to their size influence, NS has special characteristics, including enormous surface area per volume ratio and higher chemical reactivity, which triggers their ability to modify cement properties [5-8]. Many literature reports suggest that the introduction of NS into oil-well cement affects both fresh and hardened cement properties. In Pang et al.'s work, it was reported that the use of NS powders of 4–6 nm particle size would increase the compressive strength of oil-well cement by 30% and 136% within 2 and 7 days of curing respectively. The impact of nanomaterials in

* Corresponding author.
E-mail address: gujun@cug.edu.cn (G. Jun).

https://doi.org/10.1016/j.conbuildmat.2020.120393
0950-0618/

oil-well cement hydration and mechanical strength was demonstrated by Santra et al.[9] after adding NS and nanoalumina with the particle size of 30 and 140 nm respectively. They revealed that nanoparticles could stimulate the cement hydration and heighten the strength of the sheath of cement for an extended well life. In addition, NS has been found by many authors to be the best accelerator for hydration of cement and adjustment of strength [10-15].

Many researchers have grounded the effect of NS on oil-well cement properties such as setting time, compressive strength and microstructure [4,14,16,17]. These investigations acknowledged that inclusion of NS to cement slurry reduced the thickening time, increased early and late compressive strength, and refined the hardened cement microstructure by depressing porosity and permeability. Additionally, adding nanoparticles to cement speeds up the hydration process, which decreases the wait on cement (WOC) time and thus saves the hours of the rig [4,9,18]. Haruehansapong et al. recorded one of the interesting observations on nanoparticles [19]. This probe revealed that cement mortar comprising of 40 nm particle size NS showed powerful results in compressive strength compared to a test containing 12 nm particle size NS under similar curing conditions. It has been stated that 40 nm NS enhanced the strength by 54.4% compared to the control samples, while 12 nm NS particles improved the strength by 23.4%.

Numerous authors [4,20-23] have posited some potential NS mechanisms in cement. Firstly, the nano-scale size allows the use of NS as filler material by sealing the gaps in the cement matrix, creating a dense and compact structure with lessened capillary porosity. Secondly, NS powders have higher pozzolanic activity, making them the strongest cement hydration accelerators. Singh et al.[23] examined the effect of NS during hydration of cement and conclusively argued that the blending of NS into cement grains creates $H_2SiO_4^{2-}$ that reacts with the existing Ca^{2+} to produce an excess calcium silicate hydrate (C-S-H). Such C-S-H gelatin spreads in the water between the cement grains and serves as germs for further compacted C-S-H gel development. Thus, NS powders cause pozzolanic reaction.

Nonetheless, the use of NS in cement-based materials has two specific challenges. One of these problems is the dispersal of NS particles in a cement mixture. Some earlier researchers have reported that NS powders' dispersion affects the workability of cement pastes, the degree of hydration of cement and the mechanical properties of hardened cement. The preceding works concluded that the optimal NS content must be small (1–5% by weight of cement (BWOC)) to avoid agglomeration of NS particles during blending. Some researchers, however, opined that cement output can also be enhanced with higher NS replacement up to almost 10% BWOC, if NS particles are effectively dispersed in the cement. Another issue of NS particles in a cement mixture is the reduction of its slurry fluidity due to its enormous surface area and the high water demand. Several authors who investigated the contact with cement containing NS powders from dispersing agents, discovered that the form and concentration of dispersing agents together with NS particle sizes affected the rheology of the cement slurries.

As explained earlier, the strength enhancement of the specimens with NS particle size of 40 nm was considerably greater than the strength progression in samples with NS particle size of 12 nm. Thus NS particle size has conceivable effects on hardened cement's mechanical properties.

Despite extensive research on cement properties with nanoparticles over the past few years, studies on the effect of nano-scale materials of various sizes are infrequently found. The modification of properties in cement slurry containing nanoparticles of a single particle dimension has been examined by numerous researchers. Therefore, the thrust of this study is set on inspecting the effect of nanoparticle size on the early compressive strength of cement for improved oil-well integrity. In oil-well cementing, early compressive strength is significant because it precludes the leakage of formation fluids into the wellbore during the cement setting. Three different dimensions of silica nanoparticles were used. The findings produced were related to the non-NS control specimens. The scanning electron microscope, X-ray diffraction and thermogravimetric techniques were used to perform the microscopic analysis tests.

2. Experimental program

2.1. Materials

The materials used in this work were: Class G oil-well cement, corresponding to American Petroleum Institute (API) Specification 10A, (produced by Jiahua Enterprises Corp., Sichuan China, its clinker compositions are presented in Table 1), NS particles and dispersant (purchased from Guangzhou Probing Fine Chemical Co., Ltd, China. The technical specifications of the silica particles are provided in Table 2.

2.2. Experimental methods

2.2.1. Slurry preparation

The concept of cement pastes followed the API [24]. The nanoparticles (1, 2, 3 and 4% by weight of cement) were combined with the Class G Oil-well cement, and the water-to-cement ratio (W/C) was 0.45. The cement pastes were blended at a high-speed mixer (4000 r/min for 15 sec, then 12,000 r/min for 35 sec according to AP1 10A standards) [24]. An adequate amount of dispersants was added to the mixtures, in order to attain the slurry's preferred flowability. The rheological test was then conducted to determine the flowing nature of the design slurry. For this experimental work, two sets of mixtures were made. The blend CO was prepared as control samples while the NS series were produced with various contents of silica particles. The details of the cement slurry's mixing proportions are given in Table 3.

2.2.2. Early compressive strength

This research was carried out in compliance with the requirements of the API [25]. The slurry was poured into a copper mold ($5 \times 5 \times 5$ cm^3) and healed for 8, 24 and 36 h at 50 °C in an atmospheric pressure curing bath. Eventually, a pressure measurement instrument (YES-300B) was used to measure the mechanical strengths at a loading rate of 1.2 kN/s. Three specimen readings were taken to produce perfect results, and the average value was determined. Standard deviation (SD) and the Coefficients of variation (CV) were also calculated and presented with the results to ensure the quality control of the data. The lower CV indicates more accurate results while the higher CV indicates less accurate results. We calculated SD and the CV by;

$$S.D = \sqrt{\frac{\sum_{i=1}^{n}\left(X_i - \bar{X}\right)^2}{n-1}} \quad (1)$$

$$C.V = \frac{S.D}{\bar{X}} * 100\% \quad (2)$$

Where; x_i is one sample value; $\bar{X}$is the sample mean; n is the sample size

2.2.3. Rheological test

Using a ZNN-D6 rotational viscometer, manufactured by Qingdao Haitongda Equipment Corp., China, the effect of nanoparticles

Table 1
Chemical and mineral composition of Class G oil-well cement used.

Composition of Class G oil-well cement (wt %)									
SiO_2	Al_2O_3	Fe_2O_3	CaO	MgO	SO_3	C_3S	C_2S	C_4AF	C_3A
23.056	2.86	3.52	65.2	1.79	2.12	59.890	16.756	10.70	1.63

Table 2
Properties of nanoparticles.

Species	Average diameter (nm)	Color	Surface volume Ratio (m^2/g)	pH	Purity value (%)
SiO_2	10	White	220	5.7	99.9
SiO_2	20	White	90	5.7	99.9
SiO_2	40	White	50	5.7	99.9

Table 3
Mixing proportions for each experimental test.

Batch	Water (g)	Cement (g)	Nanoparticles (g)	Total weight (g)	W/C Ratio
CO 0%	354	792	0	792	0.45
NS 1%	354	784.08	7.92	792	0.45
NS 2%	354	776.16	15.84	792	0.45
NS 3%	354	768.24	23.76	792	0.45
NS 4%	354	760.32	31.68	792	0.45

on the slurry rheological properties were determined. The dial readings were recorded under different rotational speeds (θ) of 600, 300, 200, 100, 6 and 3 rpm respectively. The flow behavior index (n) and consistency coefficient (K) of the slurry was calculated as follows;

$$n = 2.096\log\left(\frac{\theta_{300}}{\theta_{100}}\right) \quad (3)$$

$$K = \frac{0.511\theta_{300}}{511^n} \quad (4)$$

Where θ_{300} is the reading at a shear rate of 300 rpm, and θ_{100} is the reading at the shear rate of 100 rpm. A larger 'n' indicates a better slurry fluidity while a larger 'K' indicates a thicker slurry.

2.2.4. Scanning electron microscopy (SEM)

The research followed SEM to analyze the hydration products and microstructures in order to investigate the morphology of the cement samples being studied. SEM analysis was performed on a Quanta200 instrument manufactured by Holland FEI (Hong Kong) Co Ltd. The back-scattered electron (BSE) imaging technique was used to analyze the specimens, which were tested under the situation to ensure their subsequent analytical capability.

2.2.5. Thermogravimetric (TG) analysis

The TG analysis was conducted using the thermal analyzer instrument's detailed STA 409 PC model. The specimens were heated in an inert atmosphere of nitrogen gas from 20 to 1000 °C with a heating rate of 20 °C/min.

2.2.6. X-ray diffraction (XRD)

To determine the phase of cement samples, a D8-Focus X-ray diffractometer (produced by Bruker AXS GmbH, Germany) was used. XRD was used to test the reduction of Portlandite during the pozzolanic activity.

3. Results and discussion

3.1. Early compressive strength

3.1.1. Effect of NS particle size on early compressive strength

Tables 4-6 summarize the early compressive strength of oil-well cement with different proportions of NS particles relative to the control specimens without NS. The effect of NS particle sizes on early compressive strength is addressed by adjusting the NS dosages. Visibly, all NS dosages strengthened the early compressive strength. The results clearly indicate that when larger sized particles were introduced into the mix, greater early compressive strength was reached. The size of NS particles therefore directly affects the early compressive strength of hardened cement. The specimens made up of 40 nm particle size NS powder provided powerful results comparable to samples containing NS particles of 10 and 20 nm. It can therefore be inferred, based on the results, that small particles of NS (10 and 20 nm) are not favorable for filling efficiency. These are conceivably glazed on the surface of the cement grains instead of the particles filling the openings within the cement grains, thereby lowering the reactivity of the cement hydration.

In addition, very tiny NS particles (10 and 20 nm) are capable of producing agglomeration and poor distribution because of their huge specific surface area. In the works of [15,19,23], these trends were established. The authors declared that the biggest challenge for all nanomaterial applications, is to obtain effective dispersion of NS into cement slurry.

The specimens made up of 40 nm particle size NS were the main early compressive power. This is because 40 nm particle dimension is an average size, an appropriate size that is very effectual in pozzolanic activation-filling effect and even distribution of particles. Therefore, early strength improvement is a result of all the effects. These discoveries also agree with the prior findings, which established that the cement composed of NS with a particle size of 10 nm, demonstrated a lower development of strength than that of cement with 40 nm particle NS dimension [19].

Table 4
Early compressive strength of hardened cement containing 10 nm NS cured at 50 °C.

Slurry batch	NS (%)	8-hours curing time			24-hours curing time			36-hours curing time		
		Mean (MPa)	SD	CV (%)	Mean (MPa)	SD	CV (%)	Mean (MPa)	SD	CV (%)
CO	0	9.67	0.44	5.0	22.66	1.76	8.0	27.02	1.02	5.0
NS10	1	11.88	0.95	10.0	25.61	1.83	9.0	28.17	1.31	6.0
NS10	2	12.94	0.92	9.0	27.33	0.99	4.0	27.60	1.03	5.0
NS10	3	13.24	1.10	10.0	28.79	1.03	4.0	32.65	0.90	3.0
NS10	4	13.15	0.62	6.0	27.98	0.69	3.0	31.58	1.55	6.0

Table 5
Early compressive strength of hardened cement containing 20 nm NS cured at 50 °C.

Slurry batch	NS (%)	8-hours curing time			24-hours curing time			36-hours curing time		
		Mean (MPa)	SD	CV (%)	Mean (MPa)	SD	CV (%)	Mean (MPa)	SD	CV (%)
CO	0	9.67	0.44	5.0	22.66	1.76	8.0	27.02	1.02	5.0
NS20	1	12.66	0.45	4.0	29.55	0.62	3.0	32.96	1.88	7.0
NS20	2	12.97	0.89	8.0	32.56	1.17	4.0	34.85	1.37	5.0
NS20	3	13.71	1.11	7.0	35.59	0.74	3.0	39.47	1.36	4.0
NS20	4	13.34	1.01	9.0	33.63	0.85	3.0	34.82	1.01	4.0

Table 6
Early compressive strength of hardened cement containing 40 nm NS cured at 50 °C.

Slurry batch	NS (%)	8-hours curing time			24-hours curing time			36-hours curing time		
		Mean (MPa)	SD	CV (%)	Mean (MPa)	SD	CV (%)	Mean (MPa)	SD	CV (%)
CO	0	9.67	0.44	5.0	22.66	1.76	8.0	27.02	1.02	5.0
NS40	1	13.78	0.82	8.0	32.64	0.89	3.0	35.14	1.43	5.0
NS40	2	15.07	0.57	4.0	35.02	0.85	4.0	37.04	1.36	4.0
NS40	3	15.37	0.76	6.0	36.85	0.85	3.0	39.82	138	4.0
NS40	4	15.00	0.48	3.0	36.04	0.92	3.0	37.22	1.76	6.0

In summary, all of the obtained results were generally in good order. As presented in Tables 4-6, the calculated CV was within an acceptable range. Nevertheless, the results show that the lowest CV was obtained from the samples containing 40 nm NS (3–8%), while the 10 nm and 20 nm particle size specimens had a CV of 3–10%. The uniform distribution of the particles in the cement slurry could be the reason why the results in the specimens with a particle size of 40 nm NS are more consistent than 10 and 20 nm NS counterparts.

3.1.2. Effect of NS particle size on the optimal dosage

Figs. 1-3 indicate the tendency of early compressive strength by correspondingly fluctuating the NS dosage for 10, 20 and 40 nm nanomaterial sizes. It describes the effect of particle size of NS on the optimal dosage. For all particle sizes and curing times of hardened cement (8, 24 and 36 h), the early compressive strength of hardened cement containing NS has been increased by the cumulative NS contents. The early compressive strength was steadily increased up to the 3% NS dose. However, after adding 4% NS,

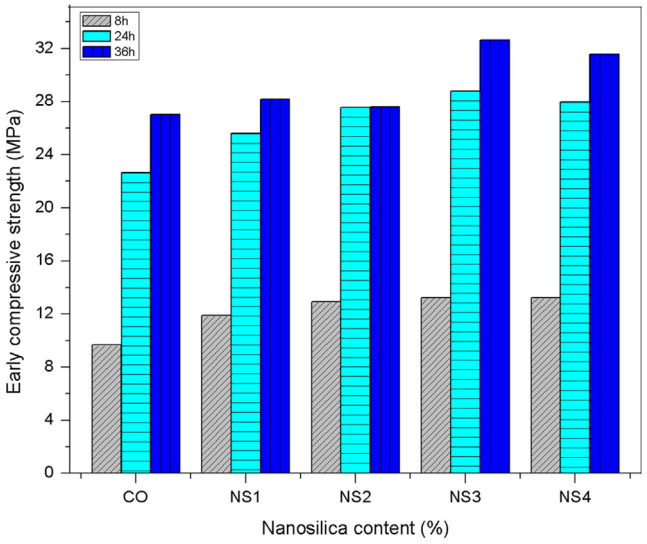

Fig. 1. Early compressive strength of hardened cement containing NS particle size of 10 nm.

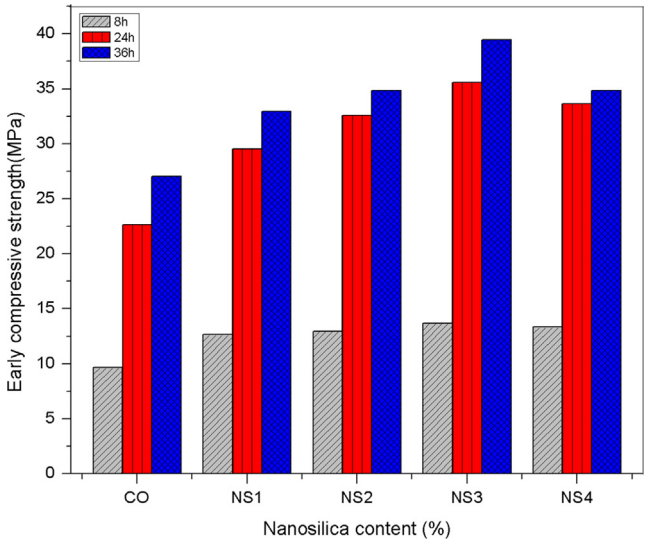

Fig. 2. Early compressive strength of hardened cement containing NS particle size of 20 nm.

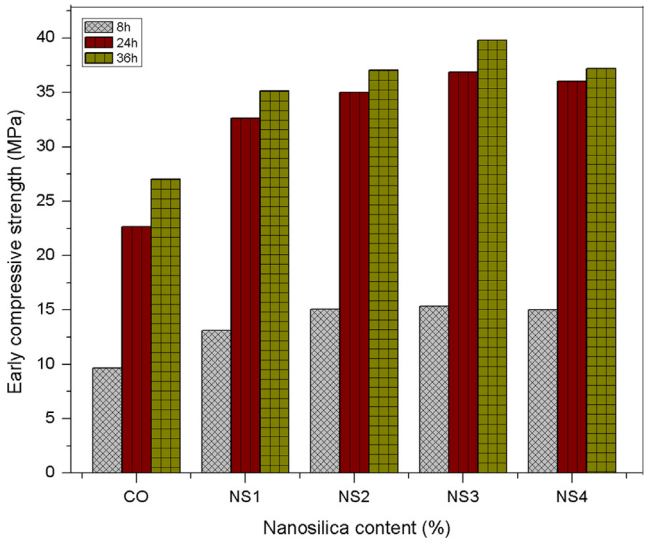

Fig. 3. Early compressive strength of hardened cement containing NS particle size of 40 nm.

the strength slightly decreased. The results of this study suggest that, the optimal amount of NS to replace the cement was 3%. This means that incorporating more or less quantity than the optimal dosage (3%) can really lessen the early strength instead of boosting it. In addition, the lower doses of NS (1 and 2%) are not sufficient to stimulate the pozzolanic reaction.

Therefore, their corresponding compressive strengths are slightly enhanced. By incorporating nano-powders in oil-well cement with extreme content (4%), the pozzolanic action will conceivably be promoted. However, the real mass of cement in the combination will concurrently be diminished, leading to inactive cement hydration. The decrease in hydration activity may have been greater than the pozzolanic reaction progressions. Therefore, lower early compressive strengths were eventually attained. The study also discovered that the overuse of NS powder in cement precludes uniform dispersal of the particles. However, the determination of the optimal content of NS in cement cannot be fixed with a definite proportion. The optimal replacement dosage of NS in cement depends on multiple factors including the type of NS which could either be dry powder or colloidal [23].

3.1.3. Effect of NS particle size on rheological properties

Tables 7-9 show the effects of NS dosages on the rheology of the oil-well cement slurry. The measurements are reported as an average of the ramp-up and ramp-down readings. The readings were reported at different rotational speeds, first in ascending order and then in descending order, and the readings showed good consistency. The results indicate that after adding NS into the cement, the apparent viscosities of the slurry at all shear rates had a slight variation. The results show that the consistency coefficient *K* rises and the fluidity index *n* declines. This indicates that the cement slurry becomes poorer after incorporating NS. The cement slurry becomes much heavier with the addition of NS. The results revealed that NS particles with higher surface area (10 and 20 nm) made the slurry much thicker than that of particle size of 40 nm.

Chithra et al. [21] established that the incorporation of NS in cement-based materials lessens the workability because part of the blending water is absorbed by NS particles. Molecules of water are freely drawn towards the NS powders due to huge surface area and higher reactivity. In addition, Bera et al. [26] examined the rheology of cement slurries and noted that the blending of NS into cement significantly raises the water requirement in the mix to maintain its workability. Such behavior indicates that the incorporation of enormous surface area particles into cement results in the high demand for water to maintain the workability of the slurry. Some authors reported that when the content of water in the mixture is preserved, increasing the content of NS would facilitate the packing of the materials.

3.2. Material characterization techniques

3.2.1. SEM analysis

Fig. 4 displays the microstructure of the control specimen without NS particles at a curing age of 14 days, where the main components are the C–H-S gels and voids with little connection between the hydration materials. The C-S-H gelation appears like a honeycomb structure, which is indeed unlike the normal C-S-H gels. As observed from the SEM image, the honeycomb gels cannot create a compact and dense cement matrix. The loose microstructure corresponds with the poor early compressive strength results, compared to samples containing NS.

Figs. 5-7 present SEM micrographs of the hardened cement with 3% NS at a curative age of 14 days, using NS particle dimensions of 10, 20 and 40 nm respectively. The images indicate that the particle dimensions of NS considerably affects the microstructure of the hardened cement. It can be visibly seen that after adding 3% of NS the main product of cement hydration is C-S-H gels in the flaky, needle and rod-like structures. The SEM images indicate that the grains of hydration products of the cement composed of 10 and 20 nm particle sizes were less uniform, compact and denser than that of NS with 40 nm particle dimension. It must be noted that particle sizes of 10 and 20 nm are excessively low for filling effect. Instead of the particles plugging the gaps between cement grains, it is plausible that they create a coat on the surface of the cement grains. This affects the hydration mechanism of the cement.

Due to the plugging effect of nano-sized particles, it was expected that a large part of the pores would be filled especially at optimal ratios of NS. However, as the SEM micrograph of cement shows, lots of voids still exist within the structure comparable to the 40 nm SEM image. The reason for this may be due to the large surface area of 10 and 20 nm particles that leads to agglomeration, preventing the uniform distribution of the particles with the cement.

As displayed in Fig. 7, the spatial structures of the hardened cement are more uniform, dense and compact, revealing the improvement of the microstructure of the hardened cement with

Table 7
Effect of NS (10 nm) on the rheological properties.

NS (%)	W/C (%)	Shear rate (rev/min)					$SD_{\theta 300}$	CV (%)	$SD_{\theta 100}$	CV (%)	n	K
		300	200	100	6	3						
0	0.45	91	78	62	21	15	3.0	5.0	3.0	7.0	0.349	5.275
1	0.45	112	87	85	19	16	5.0	6.0	6.0	10.0	0.306	8.489
2	0.45	153	124	107	25	18	5.0	5.0	5.0	7.0	0.325	10.300
3	0.45	167	137	115	29	23	7.0	6.0	5.0	6.0	0.339	10.303
4	0.45	168	140	117	32	25	7.0	6.0	7.0	6.0	0.329	11.032

Table 8
Effect of NS (20 nm) on the rheological properties.

NS (%)	W/C (%)	Shear rate (rev/min)					$SD_{\Theta 300}$	CV (%)	$SD_{\Theta 100}$	CV (%)	n	K
		300	200	100	6	3						
0	0.45	91	78	62	21	15	3.0	5.0	3.0	7.0	0.349	5.275
1	0.45	123	108	85	28	19	4.0	5.0	2.0	3.0	0.336	7.732
2	0.45	107	95	76	28	21	4.0	5.0	2.0	4.0	0.311	7.861
3	0.45	103	92	74	30	24	1.5	2.0	2.0	4.0	0.301	8.054
4	0.45	91	89	67	34	22	2.0	3.0	2.0	4.0	0.279	8.162

Table 9
Effect of NS (40 nm) on the rheological properties.

NS (%)	W/C (%)	Shear rate (rev/min)					$SD_{\Theta 300}$	CV (%)	$SD_{\Theta 100}$	CV (%)	n	K
		300	200	100	6	3						
0	0.45	91	78	62	21	15	3.0	5.0	1.0	2.0	0.349	5.275
1	0.45	96	80	66	19	16	2.0	3.0	2.0	3.0	0.341	5.849
2	0.45	91	81	64	21	16	2.0	3.0	2.0	4.0	0.320	6.321
3	0.45	89	75	63	28	18	1.0	2.0	2.0	4.0	0.314	6.417
4	0.45	90	73	64	29	20	2.0	3.0	2.0	4.0	0.310	6.654

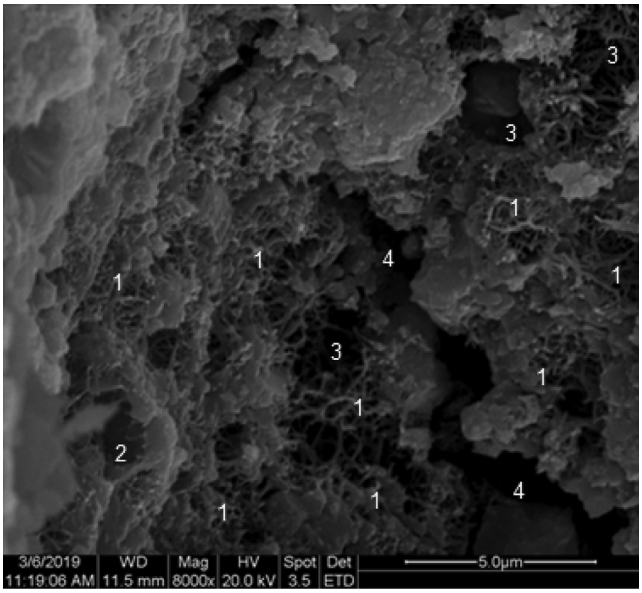

Fig. 4. SEM photograph of hardened cement without NS at a curing age of 14 days. 1 = honeycomb C-S-H gel, 2 = $Ca(OH)_2$, 3 = pores, 4 = fracture.

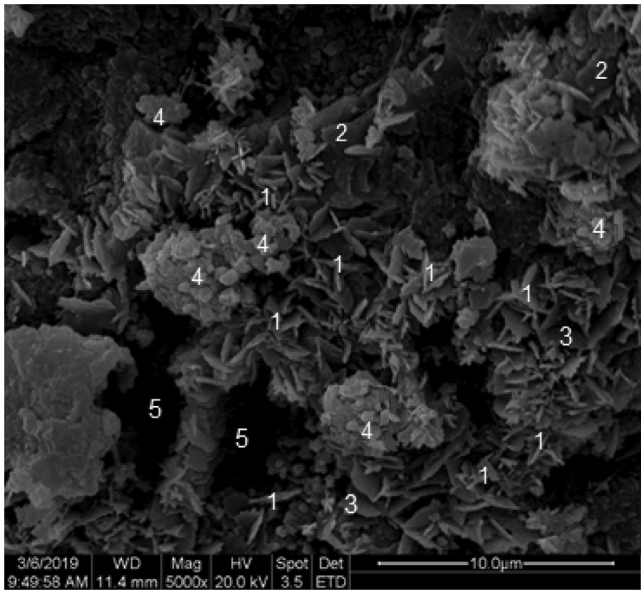

Fig. 5. SEM photograph of hardened cement having NS of 10 nm particle size at a curing age of 14 days. 1 = needle-like C-S-H gel, 2 = $Ca(OH)_2$, 3 = flaky C-S-H gel, 4 = NS particles, 5 = pores.

3% of 40 nm NS particles. It could be found that 40 nm silica nano-powders are ideal measurements for plugging gaps in the cement grains, resulting in a more compact and dense texture. Due to its surface area, 40 nm NS powders can promote the development of C-S-H gels that gather cement particles together and create stable closed structures compared to 10 and 20 nm particle sizes. Therefore, adding NS powders may increase the compressive strength of the hardened cement while altering the cement matrix microstructure.

3.2.2. TG analysis

Fig. 8 presents the TG curves of the cement incorporated with 10, 20 and 40 nm NS respectively, at a curing age of 14 days. The TG graphs indicate the usual reactions in the cement paste when exposed to a progressive thermal condition ranging from room temperature to 1000 °C. The weight loss in the cement paste specimens, occurred predominantly in three phases when exposed to rising temperatures. Firstly, at room temperature to 200 °C, the loss in mass was due to the dehydration of water molecules in cement hydration materials such as C-S-H and ettringite (calcium sulphoaluminate hydrate) [27-29]. As observed in Fig. 8, the percentage increase in weight loss indicates the increasing amount of the generated hydration materials. The effect of NS and NS particle size in stimulating cement hydration reaction was confirmed. Because of the pozzolanic nature of NS, specimens containing NS presented higher mass loss compared to control samples, indicating that more C-S-H gels were produced in samples containing NS. Nevertheless, specimens containing trivial NS particle size (10 and 20 nm) provided less mass loss compared to samples with a particle size of 40 nm. Based on the results, NS with 40 nm particle dimension, is medium-sized and very effectual in the case of

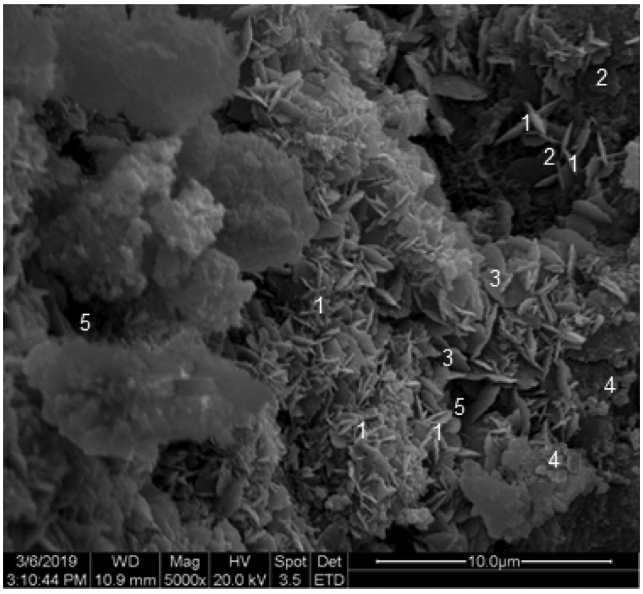

Fig. 6. SEM photograph of hardened cement having NS of 20 nm particle size at a curing age of 14 days. 1 = needle-like C-S-H gel, 2 = $Ca(OH)_2$, 3 = flaky C-S-H gel, 4 = NS particles, 5 = pores.

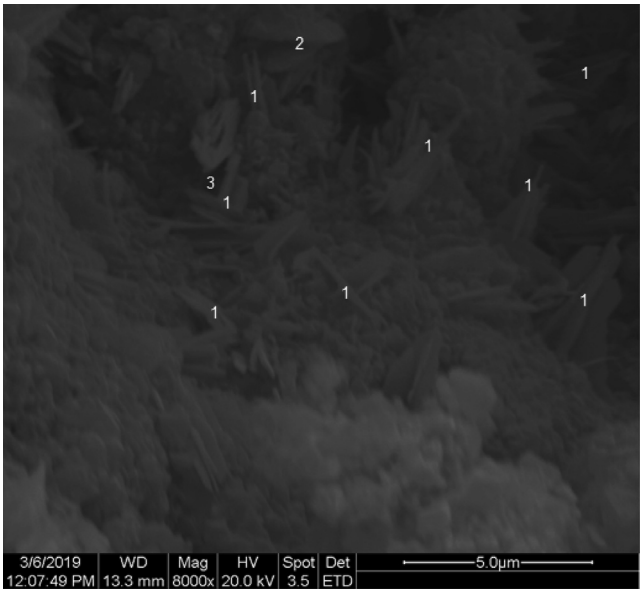

Fig. 7. SEM photograph of hardened cement having NS of 40 nm particle size at a curing age of 14 days. 1 = rod-like C-S-H gel, 2 = $Ca(OH)_2$, 3 = pores.

pozzolanic activity. This corresponds with the results of the compressive strength obtained.

The second thermal decomposition appeared between 325 and 550 °C. The corresponding weight loss in this range of temperature was due to the thermal degradation of $Ca(OH)_2$ [30-32]. The greatest mass loss at this step was seen in the control samples compared to specimens with NS. This scenario describes the role of NS as a pozzolanic agent. The pozzolanic reaction of $Ca(OH)_2$ with NS, generates additional C-S-H which is the main component of strength development in cementitious materials. In other words, this reaction converts $Ca(OH)_2$ into C-S-H gels. Therefore, the reason for the control samples to have higher percentage mass loss at this interval, is because pozzolanic reaction which reduces the level of $Ca(OH)_2$ in the hardened cement occurred only in the samples

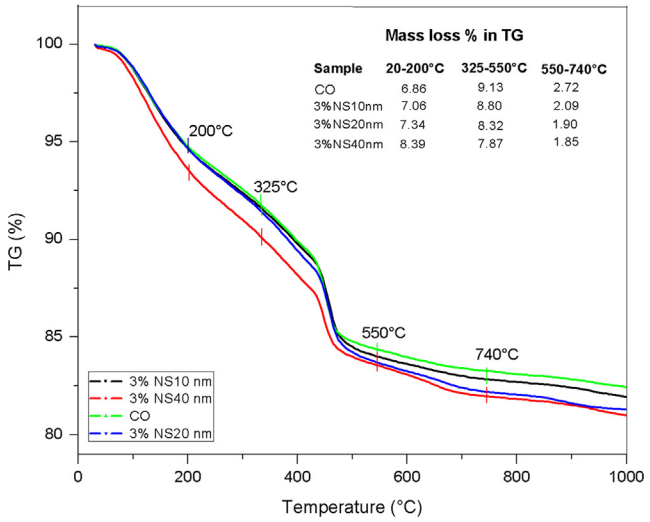

Fig. 8. TG curves of the hardened cement composed of 3% NS at a curing age of 14 days.

containing NS. On the other hand, due to efficient pozzolanic action, the specimens containing NS with a particle size of 40 nm provided the least percentage in mass loss.

The third interval of thermal decomposition occurred between 550 and 740 °C, which was due to the degradation of calcium carbonate ($CaCO_3$) and escape of carbon dioxide gas (CO_2) from the cement body. It has been established that during curing of cement, $Ca(OH)_2$ generated in the cement combine progressively with CO_2 from the surrounding to form $CaCO_3$ [33]. In this temperature range, the control samples also showed higher contents of CO_2, in comparison with the specimens composed of NS.

3.2.3. The $Ca(OH)_2$ consumption

Fig. 9 shows XRD diffractograms for NS modified cement specimens composed of 10, 20 and 40 nm particle sizes and the control samples. The consumption of Portlandite $Ca(OH)_2$ was confirmed by a 14-day XRD study following a 3% NS cement replacement. The occurrence of $Ca(OH)_2$ (CH) shows that there has been a hydration reaction, i.e. calcium silicate mixes with water to give C-S-H gel and CH. From the diffractograms, it can be seen that pure cement contains 100% of CH, and this CH content decreases depending on the size of NS in cement.

In addition, the diffractograms indicate that pozzolanic activity is significantly affected by NS particle sizes. The higher the NS surface area, the lower the $Ca(OH)_2$ consumption. The specimens containing 10, 20 and 40 nm particle sizes reduced the content of Ca $(OH)_2$ by 19.1%, 25.82% and 30.34%, respectively, at similar cement replacement (3%).

Possibly the presence of agglomerates of very small NS particles within the cement matrix, is responsible for the weak pozzolanic reactivity of the 10 and 20 nm NS particles. Since pozzolanic action can only be influenced by the outside surface of the agglomerates yet the passage of the material within the conglomerates ' thin pores is very slow, the pozzolanic reaction of the NS powders can be limited. Therefore, the clustering of nanoparticles in the cement paste is likely to be the reason for the low pozzolanic reactivity of the 10 and 20 nm specimens.

Therefore, the XRD investigation shows that NS powder with 40 nm particle size has a greater pozzolanic property than a comparable nano-powder percentage (3%) with particle sizes of 10 and 20 nm particle sizes. The XRD test results are in good agreement with the compressive strength data of the hardened cement paste.

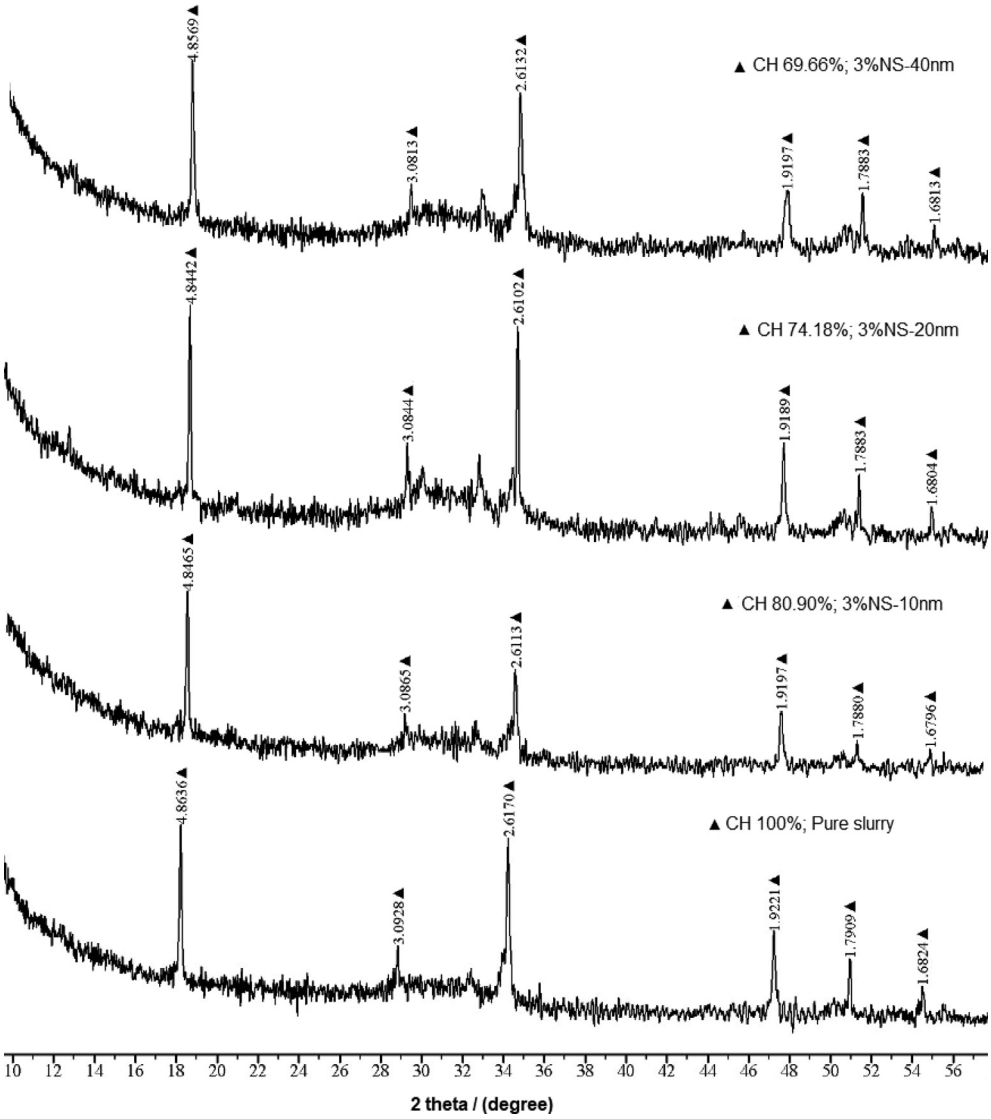

Fig. 9. XRD cement diffractograms showing CH consumption with and without NS at a curing age of 14 days.

4. Conclusions

In this study, NS with dissimilar particle sizes (10, 20 and 40 nm) was selected to investigate the influence of nanoparticle sizes on early compressive strength of oil-well cement. Based on the results, the following statements are drawn;

1. The findings demonstrate that particle size affects the early compressive strength of oil-well cement. The 40 nm particle size provided the highest compressive strength equivalent to 10 and 20 nm particle size NS specimens. The plausible reason is poor distribution and agglomeration of very tiny particles in cement.
2. NS powders stimulate the cement hydration by generating C-S-H gels through the reaction with $Ca(OH)_2$. Therefore, NS provides both pozzolanic activity and filling capabilities.
3. The optimal dosage of NS particles in cement was found to be 3% for this study. Overuse of NS results in particle agglomeration and reduction in early compressive strength.
4. SEM images revealed that NS powders can modify the microstructure of hardened cement, making the structure more compact and denser, on condition that the content of NS is appropriate and evenly distributed.
5. The pozzolanic reactivity of NS was confirmed by monitoring the variation of the quantity of $Ca(OH)_2$ and $CaCO_3$ from the second and third intervals of the TG analyses. The pozzolanicity test was also presented by the XRD report. NS with 40 nm particle size was medium-sized; and provided the best results in terms of pozzolanic activity.

CRediT authorship contribution statement

Mtaki Thomas Maagi: Conceptualization, Methodology, Software, Data curation, Formal analysis, Writing - original draft. **Gu Jun:** Supervision, Validation, Writing - review & editing.

Declaration of Competing Interest

The authors declare that they have no known competing financial interests or personal relationships that could have appeared to influence the work reported in this paper.

Acknowledgments

This work was supported by the National Natural Science Foundation of China (grant no. 41972326 and 51774258).

References

[1] N. Agbasimalo, M. Radonjic, Experimental study of the impact of drilling fluid contamination on the integrity of cement-formation interface, J. Energy ResTech 136 (2014).
[2] M. Radonjic, A. Oyibo, Experimental Evaluation of Wellbore Cement-Formation Shear Bond Strength in Presence of Drilling Fluid Contamination, 5th International Conference on Porous Media and Their Applications in Science, Engineering and Industry, Eds, ECI Symposium Series, (2014).
[3] E.B. Nelson D. Guillot Well Cementing 2006 Developments in Petroleum Science Book Series Schlumberger
[4] M.F. Fakoya, S.N. Shah, Emergence of nanotechnology in the oil and gas industry: Emphasis on the application of silica nanoparticles, Petroleum, 3 (2017) 391-405.
[5] M. Amanullah, A.M. Al-Tahini, Nanotechnology- its significance in smart fluid development for oil and gas field, SPE Saudi Arabia Section Technical Symposium, SPE, 2009.
[6] R. Patil, A. Deshpande, Use of nanomaterials in cementing applications, SPE, SPE International Oilfield Nanotechnology Conference and Exhibition, 12–14 June, Noordwijk, The Netherlands, 2012.
[7] L. Senff, D. Hotza, W.L. Repette, Rheological characterization of cement pastes with nanosilica, silica fumes and superplasters additions, Adv. Appl. Ceram. Struct. Funct. Bioceram. 109 (2010) 213–218.
[8] M. Stefanidou, Influence of nano-SiO2 on the portland cement pastes, Compos. B Eng. 43 (2012) 2706–2710.
[9] A.K. Santra P. Boul X. Pang Influence of Nanomaterials in Oilwell Cement Hydration and Mechanical Properties 2012 The Netherlands SPE International Oilfield Nanotechnology Conf & ExhNoordwijk 13
[10] J.J. Gaitero, I. Campillo, A. Guerrero, Reduction of the Calcium Leaching Rate of Cement Paste by Addition of Silica Nanoparticles, Cem. Concr. Res. 38 (2008) 1112–1118.
[11] D. Kong, X. Du, S. Wei, Influence of nano-silica agglomeration on microstructure and properties of the hardened cement-based materials, Constr. Build. Mater. 37 (2012) 707–715.
[12] D. Kong, Y. Su, X. Du, Influence of nano-silica agglomeration on fresh properties of cement pastes, Constr. Build. Mater. 43 (2013) 557–562.
[13] F. Kontoleontos, P.E. Tsakiridis, A. Marinos, Influence of colloidal nanosilica on ultrafine cement hydration Physiochemical and Microstructural characterization, Constr. Build. Mater. 25 (2012) 347–360.
[14] N. Nabhani, M. Emami, T.A.B. Moghadam, Application of Nanotechnology and Nanomaterials in Oil and Gas Industry, The 4th Nanoscience and Nanotechnology Symposium. AIP Conf, Proc, 2011, pp. 128-131.
[15] C. Wang, X. Chen, X. Wei, R. Wang, Can nanosilica sol prevent oil-well cement from strength retrogression under high temperature?, Constr. Build. Mater. 144 (2017) 574–585.
[16] A.I. El-Diasty, A.M.S. Ragab, Applications of Nanotechnology in the oil& gas industry: Latest trends Worldwide & Future Challenges in Egypt, North Africa, Tech. Conf. & ExhCairo Egypt (2013).
[17] V. Ershadi, T. Ebadi, A.R. Rabani, L. Ershadi, H. Soltanian, The effect of nanosilica on cement matrix permeability in oil-well to decrease the pollution of the receptive environment, Int. J. Environ. Sci. Dev. 2 (2011) 128–132.
[18] J.Z. Chong, N.M. Sutan, I. Yakub, Characterization of the early pozzolanic reaction of calcium hydroxide and calcium silicate hydrate for nanosilica modified cement paste, UNIMAS E-J. Civil Eng 4 (2012) 6–10.
[19] S. Haruehansapong, T. Pulngern, S. Chucheepsakul, Effect of the particle size of nanosilica on the compressive strength and the optimum replacement content of cement mortar containing nano-SiO2, Constr. Build. Mater 50 (2014) 471–477.
[20] N. Agbasimalo Experimental Study of the Effect of Drilling Fluid Contamination on the Integrity of Cement-Formation Interface MSc Thesis 2012 Department of Pet Eng, Louisiana State University USA.
[21] S. Chithra, K.S. Senthil, K. Chinnaraju, The Effects of Colloidal Nanosilica on Workability Mechanical and Durability Properties of High-Performance Concrete with Copper Slag as partial fine aggregate, Constr. & Build. Mater. 113 (2016) 794–804.
[22] G.R. Khayati, H.M. Ghasabe, M. Karfarma, A survey on the application of oxide nanoparticles for improving concrete processing, Adv. Concr. Constr. 3 (2015) 145–159.
[23] L.P. Singh, S.R. Karade, S.K. Bhattacharyya, M.M. Yousuf, S. Ahalawat, Beneficial role of nanosilica in cement-based materials-A review, Constr. & Build. Mater. 47 (2013) 1069–1077.
[24] API10A, Specification for cement and materials for well cementing American Petroleum Institute, 24th edition (2010).
[25] StatNano, Nanotechnology Publications of 2018 https://statnano.com (2019).
[26] M. Berra, F. Carassiti, T. Mangialardi, Effects of nanosilica addition on workability and compressive strength of portland cement pastes, Constr. Build. Mater. 35 (2012) 666–675.
[27] S.A. Abo-El-Enein, S.M.A. El-Gamal, I.A. Aiad, M.M. Azab, O.A. Mohamed, Early hydration characteristics of oil well cement pastes admixed with newly prepared organic admixture, HBRC (2016).
[28] L.P. Esteves, On the hydration of water-entrained cement-silica systems, combined SEM XRD and thermal analysis in cement paste, Thermochim. Acta 518 (2011) 27–35.
[29] J.I. Tobon, J.J. Paya, M.V. Borrachero, Mineralogical evolution of Portland cement blended with silica nanoparticles and its effects on mechanical strength, Constr. Build. Mater. 36 (2012) 736–742.
[30] K.J. Krakoiak, J.J. Thomas, S. Musso, S. James, A.T. Akono, F.J. Ulm, Nano-chemo-mechanical signature of conventional oil-well cement systems: effect of elevated temperature and curing time, Cem. Concr. Res. 67 (2015) 103–121.
[31] M. Frias, J. Cabrera, Influence of MK on the reaction kinetics in MK/lime and MK-blended cement systems at 20°C, Cem. Concr. Res. 31 (2001) 519–527.
[32] Y. Mleza, M. Hajjaji, Microstructural characterization and physical properties of cured thermally activated clay-lime blends, Constr & Build Mater 26 (2012) 226–232.
[33] C.F. Chang, J.W. Chen, The experimental investigation of concrete carbonation depth, Cem. Concr. Res. 36 (2006) 1760–1767.